Title

Clumped-Isotope Constraints On Cement Paragenesis In Septarian ConcretionsCEMENT PARAGENESIS IN SEPTARIAN CONCRETIONS

Journal

Journal of Sedimentary Research, 84(12)

ISSN

1527-1404

Authors

Loyd, Sean J
Dickson, JAD
Boles, James R
et al.

Publication Date

2014-12-01

DOI

10.2110/jsr.2014.91

Peer reviewed

Journal of Sedimentary Research

Journal of Sedimentary Research, 2014, v. 84, 1170–1184
Research Article
DOI: http://dx.doi.org/10.2110/jsr.2014.91

CLUMPED-ISOTOPE CONSTRAINTS ON CEMENT PARAGENESIS IN SEPTARIAN CONCRETIONS

SEAN J. LOYD,[1,2] J.A.D DICKSON,[3] JAMES R. BOLES,[4] AND ARADHNA K. TRIPATI[2]

[1]*Department of Geological Sciences, California State University, Fullerton, 800 North State College Boulevard, Fullerton, California 92834, U.S.A*
[2]*Department of Earth, Planetary, and Space Sciences, University of California, Los Angeles, 595 Charles Young Drive East, Los Angeles, California 90095, U.S.A*
[3]*Department of Earth Sciences, University of Cambridge, Downing Street, Cambridge, U.K*
[4]*Department of Earth Sciences, University of California, Santa Barbara, Santa Barbara, California 93106, U.S.A*
e-mail: ripple@ess.ucla.edu

ABSTRACT: **Septarian concretions exhibit multiple generations of cements that include body, fringe, and spar phases. Classic paragenetic interpretations include initial precipitation of the body followed by fringe(s) and then by spar in more or less discrete events. Traditional approaches (e.g., carbon and oxygen isotope analyses) are generally unable to distinguish paragenetic trends as they relate to specific formation environments (e.g., precipitation during burial or with meteoric influx). Here we present carbonate clumped-isotope, $\delta^{13}C$ ($\delta^{13}C_{carb}$), and $\delta^{18}O$ ($\delta^{18}O_{carb}$) values for septarian concretions taken from four host units in order to assess cement paragenesis and overcome traditional shortcomings. Clumped-isotope and $\delta^{18}O_{fluid}$ data exhibit a wide range of values, with carbonate precipitation temperatures between ~ 20 and 50°C and $\delta^{18}O_{fluid}$ compositions of ~ −14 to +4‰ (VSMOW). In stable-isotope cross-plots, specific cement phases group together and confirm the paragenesis indicated by superposition. In some cases, samples analyzed from concretion bodies yield temperature and $\delta^{18}O_{fluid}$ values that indicate formation at shallow depths, consistent with independent data (e.g., high minus-cement porosity, external laminae deflection). In contrast, other concretion-body analyses indicate relatively high body temperatures that conflict with shallow-formation indices. Petrographic and backscatter scanning electron microscopy (SEM) reveal that concretion bodies partially consist of a secondary, replacement phase, which could explain the higher temperatures expressed in bulk body samples. Based on data for different phases in these septarian concretions, we suggest that initial body-cement precipitation occurred at relatively shallow depths from unmodified seawater, followed by fringe formation at elevated temperatures that likely coincided with the emplacement of the secondary body phase. When considered together, late-stage spar phases exhibit temperatures and $\delta^{18}O_{fluid}$ values supportive of spar precipitation from fluids with a significant meteoric component, possibly during uplift.**

INTRODUCTION

Carbonate concretions have long been used as geochemical archives for pore-water chemistry. Analyses of concretion cements can provide insight into evolving pore-water chemistry and burial diagenesis in clastic sediments (e.g., Coleman 1993; Mozley and Burns 1993), preserving a record of conditions associated with sediment burial and cement precipitation. As such, our understanding of microbial and diagenetic processes that degrade organic matter has been strongly influenced by the study of concretions (e.g., Irwin et al. 1977; Mozley 1996).

Carbonate concretions can adopt two end-member modes of growth (Raiswell and Fisher 2000). One mode is concentric—where pores are completely filled progressively from the core to the periphery (e.g., Newberry 1873; Tomkeieff 1927; Clifton 1957; Raiswell 1971; Berner 1980; Criss et al. 1988; Coleman 1993). The second mode is pervasive—where pores throughout the final volume of the concretions are incrementally filled (Hennessy and Knauth 1985; Mozley 1989; Feistner 1989; Mozley 1996; Raiswell and Fisher 2000). In many cases, hand-sample and transmitted-light-microscopic examination of concretion body cements reveal uniformly crystalline and homogeneous textures regardless of growth style (concentric or pervasive), confounding genetic interpretations.

Concretions sometimes exhibit septarian morphologies and may contain body, fringe, and spar phases. The body is a mixture of the original sediment and finely crystalline cement and generally appears gray in color, whereas the fringe is the first filling of the septarian cracks (grown along the wall) and is composed of fibrous crystals that are often dark brown or yellow in color. Spar fills the center of the cracks and is composed of coarsely crystalline calcite that is yellow or transparent (Fig. 1). The body is classically interpreted as forming near the sediment–water interface, and the fringe and spar are interpreted as formed in open voids (e.g., Thyne and Boles 1989).

The geometries of the septarian voids can vary but often display a symmetrical morphology with the largest void volume occurring in the concretion center and tapering to lesser volume toward the periphery. Relatively straight or regular edges of internal voids have led to genetic interpretations centered on internal stress-induced (Astin 1986; Selles-Martinez 1996; Hounslow 1997), synsedimentary earthquake-induced (Pratt 2001), and/or shrinkage (Duck 1995; Hendry et al. 2006) cracking. Regardless of the specific reason for internal cracking, the superposition of cements seemingly provides a straightforward paragenetic sequence of cement precipitation. This sequence progresses sequentially from concretion body to isopachous fringe(s) to void filling spar(s). Unclear

Published Online: December 2014
 1527-1404/14/084-1170/$03.00

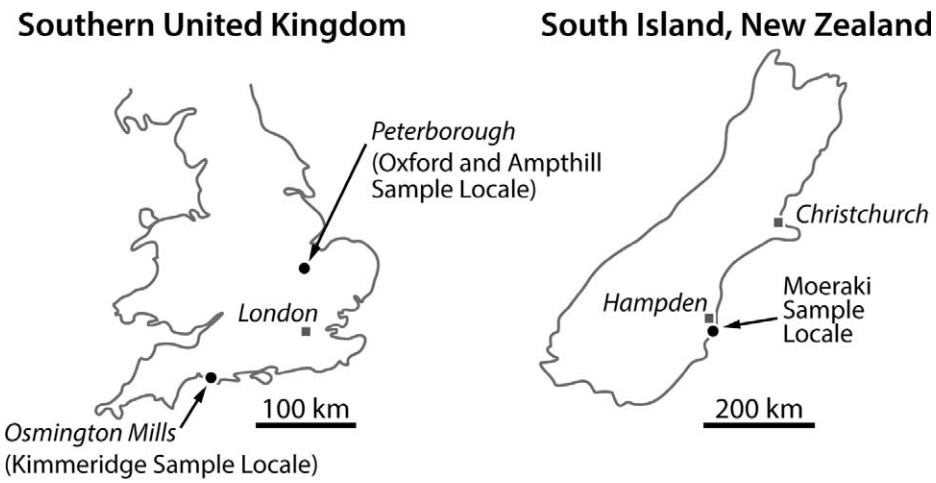

FIG. 1.—Sample locations of septarian concretions.

from this simplified paragenetic sequence is the absolute temporal relationships among phases; therefore it is impossible to quantify, for example, the amount of time that passed between fringe and spar precipitation.

Geochemical analyses of septarian concretions have generally yielded highly variable results, particularly in trace-metal concentrations, carbonate $\delta^{13}C$ ($\delta^{13}C_{carb}$), and carbonate $\delta^{18}O$ ($\delta^{18}O_{carb}$), reflecting precipitation in multiple, chemically distinct diagenetic regimes (e.g., Hyde and Landy 1966; Raiswell 1971; Hudson 1978; Marshall 1982; Gautier 1982; Gautier and Claypool 1984; Dix and Mullins 1987; Boles et al. 1985; Siegel et al. 1987; Thyne and Boles 1989; Desrochers and Al-Aasm 1993; Hudson et al. 2001; Hendry et al. 2006). Many interpretations rely heavily on $\delta^{18}O_{carb}$; but as with all carbonate minerals, interpretation of $\delta^{18}O_{carb}$ values is confounded due to the influences of both temperature and fluid $\delta^{18}O$ ($\delta^{18}O_{fluid}$) (Urey 1947). Typically the youngest cements in septarian concretions have the lowest $\delta^{18}O_{carb}$ values, which have been interpreted in three different ways. In some cases, they have been interpreted to reflect precipitation as late-stage cements during burial diagenesis (Mozley 1996; Raiswell and Fisher 2000). A second model that has been proposed invokes precipitation from relatively warm fluids that are hydrothermal in origin (Astin and Scotchman 1988). A third model suggests that septarian infill growth occurs at shallow depths from mixtures of meteoric and marine fluids (Thyne and Boles 1989; Coniglio et al. 2000; Hudson et al. 2001; Hendry et al. 2006).

A new tool, the clumped-isotope paleothermometer (Ghosh et al. 2006a), provides a means for testing these models, in that it allows for direct quantification of carbonate precipitation temperatures as well as $\delta^{18}O_{fluid}$. Clumped isotopes have proven useful in many applications, including climate reconstructions (Came et al. 2007; Tripati et al. 2010; Passey et al. 2010; Finnegan et al. 2011), paleoaltimetry studies (Ghosh et al. 2006b; Huntington et al. 2010), diagenesis (Bristow et al. 2011; Huntington et al. 2011; Loyd et al. 2012a; Dale et al. 2014), ancient faunal body temperatures (Eagle et al. 2010, 2011), and crustal cooling rates (Passey and Henkes 2012). Loyd et al. (2012a) recently applied this approach to non-septarian concretions of the Monterey Formation and Holz Shale of California and developed more precisely characterized diagenetic histories. Dale et al. (2014) present clumped-isotope data from septarian concretions of the Mancos Shale (Colorado, USA) and construct a detailed and variable diagenetic evolution. Here, we apply the clumped-isotope paleothermometer to extensively studied septarian concretions from England and New Zealand (Fig. 1) in order to constrain the diagenetic environments of concretion development.

GEOLOGIC CONTEXT

The concretions analyzed in this study were collected from the Middle and Upper Jurassic Oxford, Ampthill, and Kimmeridge Clays of central England and the Paleocene Moeraki Formation of eastern New Zealand (Fig. 1). All of the concretions exhibit textures and morphologies common in septarian concretions, including conspicuous internal veins filled with multiple generations of pore-occluding calcite cements (Figs. 2, 3). The Oxford and Ampthill Clay concretions were collected from a brick quarry (formerly owned by the London Brick Company) in Norman Cross, near Peterborough, England. The Oxford Clay concretions were collected from the base of the Oxford Clay (see Duff 1975 and Hudson 1978, for stratigraphic sections) where the unit is composed mainly of olive gray, bituminous shale. The unit contains well-preserved fauna that, along with high organic carbon contents are evidence for relatively low oxygen contents near the sediment–water interface (Duff 1975; Morris 1980). The Ampthill concretion was collected from the same quarry and sourced from an overlying Pleistocene till (similar to concretions examined in Hudson 1978). The Ampthill Clay is composed of pale to dark gray, locally burrowed mudstone. The unit is relatively thin (~ 50 m thick) and poorly exposed in outcrop. The most detailed description of the Ampthill Clay is based on recovered cores (see Cox et al. 1994, for stratigraphic section and core log). The Kimmeridge Clay concretion was collected from the base of the unit (see Scotchman 1991, for stratigraphic section) from coastal outcrops near Osmington Mills, Dorset, England. The Kimmeridge Clay is a transgressive, organic-rich and calcareous mudstone deposited under oxic to anoxic bottom waters (Gallois and Cox 1976; Irwin 1979a, 1979b; Tyson et al. 1979; Scotchman 1984; Wignall and Myers 1988; Wignall 1989). The Moeraki concretion was collected from Moeraki Formation outcrop approximately 3 km south of Hampden, New Zealand. The Moeraki Formation consists of mudstone interpreted to have formed during marine transgression. The concretions (classically referred to as ''Moeraki Boulders'') are concentrated near the middle of the Moeraki Formation (see Thyne and Boles 1979, for stratigraphic section) and are largely exposed in wave-eroded lag deposits on the beach.

METHODS

The septarian concretions were slabbed, polished (Fig. 2), and thin-sectioned (Figs. 3, 4). Polished samples were examined with a LEO 14030VP scanning electron microscope (SEM) with backscatter imaging capability (Fig. 4), an approach proven beneficial for recognizing multiple phases in concretions that could not be otherwise identified via

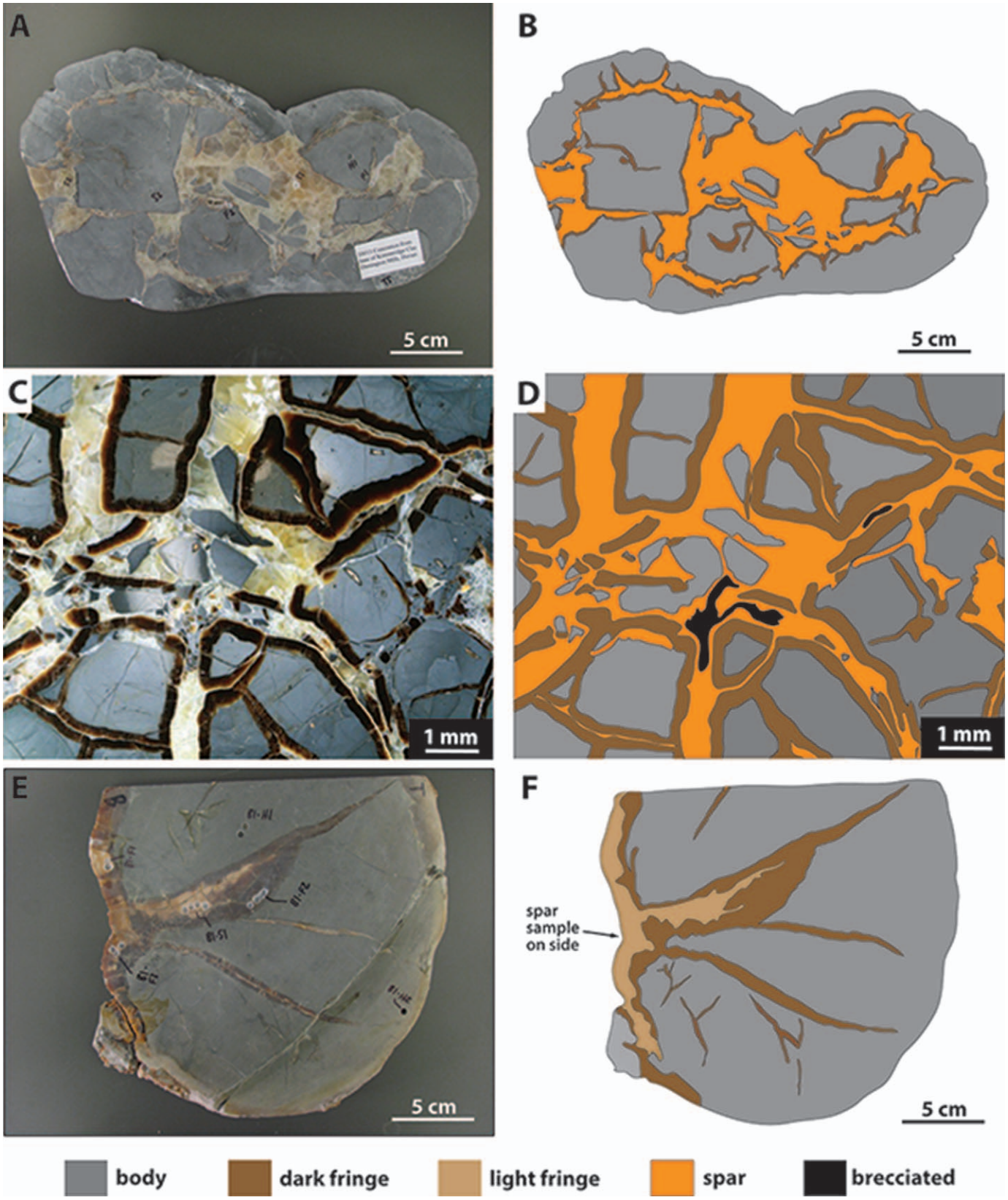

FIG. 2.—Photographed slabs and diagrams of some of the septarian concretions analyzed in this study from: **A**, **B)** the Kimmeridge Clay; **C**, **D)** the Oxford Clay; **E**, **F)** the Moeraki Formation, New Zealand.

traditional petrographic microscopy (Mozley 1996; Raiswell and Fisher 2000). Distinct phases were sampled (via drilling) for simultaneous analyses of $\delta^{18}O_{carb}$, $\delta^{13}C_{carb}$ and clumped isotopes (see Table 1 for geochemical data. Note: additional data were collected from septarian concretions from Pueblo, Colorado and Santa Barbara, California, USA, but due to inadequate geologic context, these data are provided in supplementary material only (Supp. Table 1) and not discussed here).

Clumped-Isotope Analyses

Carbonate "clumped-isotope" thermometry is based on the relative abundance of the $^{13}C^{18}O^{16}O$ (mass 47) isotopologue in CO_2 produced by acid digestion of carbonate minerals. Fractionation during acid digestion is ca. 0.2 per mil (‰) and varies predictably according to reaction temperature (Ghosh et al. 2006a; Passey et al. 2010). The abundance of the mass 47 species is reported as Δ_{47} values, representing the enrichment of this species in CO_2 relative to the stochastic distribution of isotopologues, in units of ‰ (Wang et al. 2004). Specifically Δ_{47} is defined as

$$\Delta_{47} = \left[\frac{R^{47}}{2R^{13}\cdot R^{18} + 2R^{17}\cdot R^{18} + R^{13}\cdot\left(R^{17}\right)^2} - \frac{R^{46}}{2R^{18} + 2R^{13}\cdot R^{17} + \left(R^{17}\right)^2} - \frac{R^{45}}{R^{13} + 2R^{17}} + 1\right]\cdot 1000 \quad (1)$$

where R refers to the ratio of the minor isotopologue to the major isotopologue of the molecule (or atom) of interest (i.e., $R^{13} = {}^{13}C/{}^{12}C$; $R^{17} = {}^{17}O/{}^{16}O$; $R^{47} = {}^{13}C^{18}O^{16}O/{}^{12}C^{16}O^{16}O$, etc.).

Analyses were conducted on specially modified Thermo Fisher 253 gas-source mass spectrometers dedicated to measuring clumped isotopes in CO_2. Calcite samples and standards were converted to CO_2 using a custom-built automated system for digestion and purification (after Passey et al. 2010). The automated digestion system is composed of 1) a Costech Zero Blank autosampler, 2) a common, phosphoric acid bath, 3) cryogenic traps for the purification and collection of CO_2, 4) a ThermoFinnegan Trace GC Ultra gas chromatograph, 5) additional cryogenic traps to separate prepared gases from helium carrier gas, and 6) a final set of valves and traps to purify CO_2 and transfer it to the mass spectrometer.

In this system, between 4 and 12 mg of sample is digested at 90°C for 20 minutes in oversaturated phosphoric acid (density = 1.92 g/ml) in order to ensure 1) a sufficient amount of CO_2 for stable voltages over the course of several hours and 2) minimize water production through sample digestion. The acid bath was changed after 10–15 analyses. Upon transfer to the mass spectrometer (after purification, see above), the sample gas was analyzed for masses 44 to 49 atomic mass units. Measurements are made to yield a stable 16-volt signal for mass 44, with peak centering, background, and pressure balancing before each acquisition. These conditions were selected to ensure stable ion currents and minimize time-dependent fractionation of sample and reference-gas reservoirs. The total analysis time (including peak centering, background measurement, and pressure balancing) ranged from between 4 and 8 hours. The presence of organics can yield significant isobaric interferences with CO_2 isotopologues that can impact both accuracy and precision, resulting in an apparent temperature bias and/or larger internal errors. Concretionary carbonate can contain appreciable organic carbon, and therefore masses 48 and 49 were monitored in order to assess the potential for organic contamination, although mass 49 was/is commonly below detection.

"Heated gases" with different bulk isotope compositions and 25°C water-equilibrated gases were analyzed to establish internal gas lines. To produce stochastic gasses, CO_2 samples with different bulk $\delta^{18}O$ and $\delta^{13}C$ ratios were heated in quartz breakseals are heated to 1000°C for two hours and then quenched at room temperature. Approximately two to four sample analyses and three standard analyses (both gas standards and carbonate standards) were performed each day. All standard gases are then purified and analyzed using the same protocol as for sample gases. The standard error of Δ_{47} values is reported in factors in the equilibrated gas line uncertainty.

Calculations

An empirically derived acid digestion fractionation correction of 0.08‰ (Passey et al. 2010) was applied to raw Δ_{47} values to facilitate comparison of our 90°C reactions to the published calcite line calibration in which samples were reacted at 25°C (Ghosh et al. 2006a). The data reported here are presented in the absolute reference frame (ARF) of Dennis et al. (2011) and the temperature calibration of Ghosh et al. (2006a) for inorganic calcite (as recalculated in Dennis et al. 2011) is used to convert Δ_{47} values to temperature. The use of another published temperature calibration (Dennis and Schrag 2010) does not have a substantial impact on the offsets in temperatures between cement phases or affect our conclusions.

The value used for calculating calcite $^{18}O/^{16}O$ ratios from analyzed CO_2 is 1.00821 for samples digested at 90°C (Swart et al. 1991). For calculations of equilibrium $^{18}O/^{16}O$ ratios in calcite (and to calculate $\delta^{18}O$-calcification temperatures), we used the published relationship of Kim and O'Neil (1997) to describe calcite-water fractionation:

$$1000\ln\alpha_{calcite-H_2O} = \frac{18.03\times 10^3}{T} - 32.42 \quad (2)$$

where T is temperature in Kelvin.

Accuracy and Precision

Measured Δ_{47} values for an in-house Carrara Marble standard are 0.397‰, a Carmel Chalk standard is 0.687‰, and a TV01 standard is 0.714‰. Average reproducibility of standard and sample Δ_{47} values is 0.010‰, and the reproducibility of $\delta^{13}C$ and $\delta^{18}O$ is better than 0.009‰. $\delta^{18}O_{carb}$ and $\delta^{13}C_{carb}$ values are reported in ‰ relative to the VPDB standard. Reconstructed $\delta^{18}O_{fluid}$ values are reported compared to the VSMOW standard.

RESULTS

Concretion Petrography and Morphology

British Septarian Concretions.—One concretion from the Kimmeridge Clay, two concretions from the Ampthill Clay, and one concretion form the Oxford Clay, UK, were examined (see Table 1). Although originating from three different geologic formations (all Jurassic in age), these stratigraphically adjacent units exhibit similar cement phases. Body cements are mainly micritic, contain disseminated patches of pseudospar (classification after Bathurst 1975) and are composed of an anhedral interlocking mosaic (Fig. 4). Backscatter imaging of concretion bodies reveals an electron-light and an electron-dark phase. The dark phase constitutes up to ~ 10% of the total body cement, exhibits straight-edged boundaries, and "floats" in the electron-light body phase (Fig. 4). In general, columnar isopachous fringe cements grow off of body cements. The fringe ranges from dark brown to yellowish in color and can display a systematic lightening away from the sharp host-fringe contact. Fringe thickness typically varies between ~ 100 and 500 μm. Spar cements consist of white to yellow colored, blocky crystals up to ~ 1 cm across. These spar cements fill in the remaining pore space. Both the fringe and spar phases appear homogeneous under backscatter SEM, in contrast to the body cements.

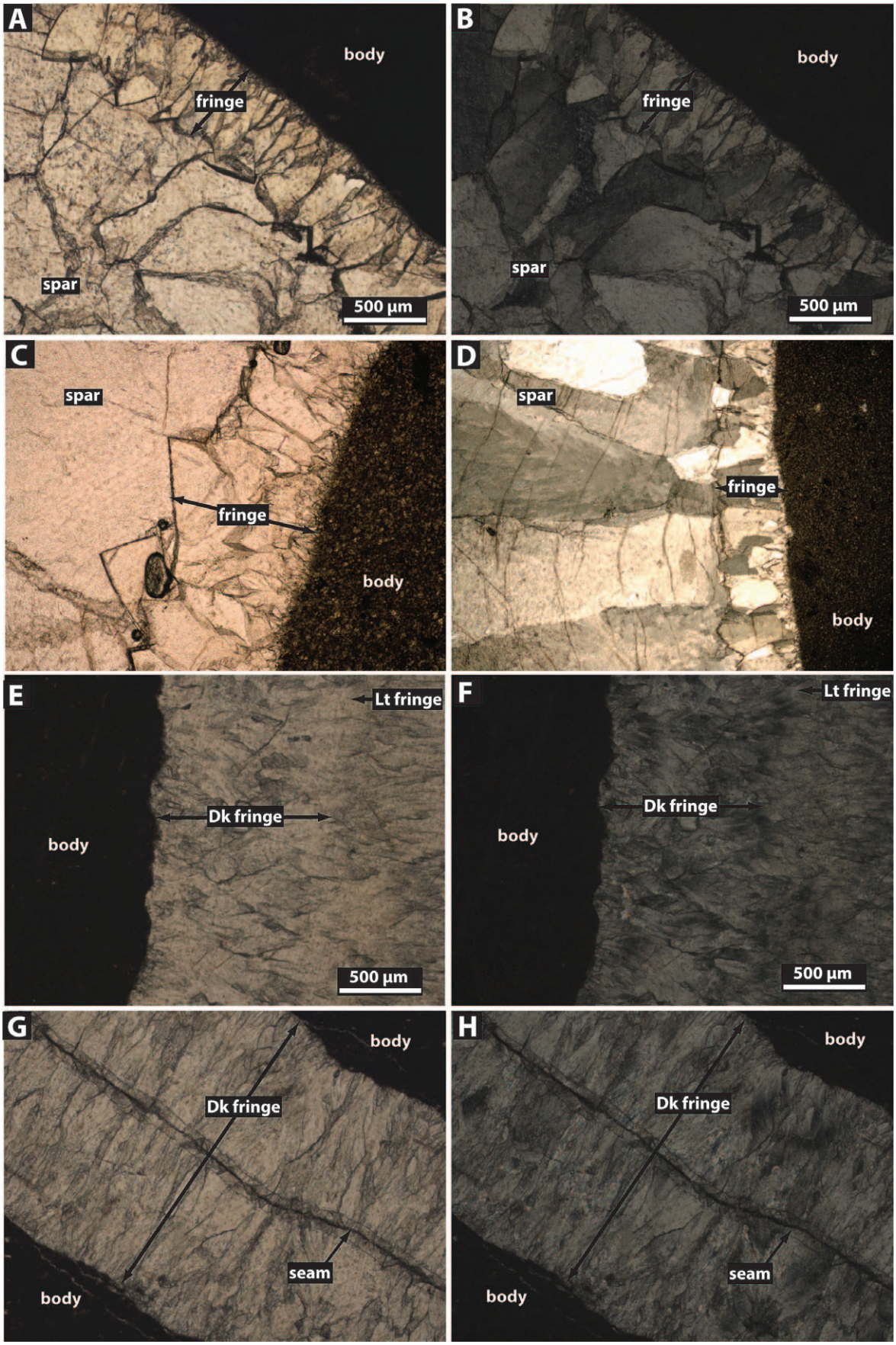
A
body
fringe
spar
500 µm
B
body
fringe
spar
500 µm
C
spar
fringe
body
D
spar
fringe
body
E
Lt fringe
Dk fringe
body
500 µm
F
Lt fringe
Dk fringe
body
500 µm
G
body
Dk fringe
seam
body
H
body
Dk fringe
seam
body

Moeraki Formation Septarian Concretion.—Body cements in this concretion are dominantly micritic and contain patches of disseminated pseudospar. Backscatter SEM imaging reveals two dominant body phases. As with the previous concretions, an electron-dark phase occurs as straight-edged "blocks" completely surrounded by electron-light body cement. The dark phases constitute ~ 15% of the entire body. Pyrite framboids up to ~ 100 μm in diameter and disseminated pyrite crystals appear bright white under backscatter SEM. Fringes generally occur as either dark brown (dark fringe) or yellow columnar isopachous, radiating and botryoidal cements (light fringe). Brown fringes are most common and grow directly off of the body cement. Where present, the yellow fringe follows the brown fringe, and the contact between the two is jagged and discontinuous. The thickest fringes (combined brown and yellow phases) are up to ~ 2 cm thick and occur as the dominant pore-occluding phase in thinner veins. In the center of larger veins, a yellow blocky calcite spar fills remaining void space. Fringe and spar phases appear homogeneous under backscatter SEM.

Geochemistry of Septarian Concretion Phases

As has been recognized in many concretions, $\delta^{13}C_{carb}$ and $\delta^{18}O_{carb}$ values vary considerably among phases (Fig. 5). Where available, previously reported $\delta^{13}C_{carb}$ and $\delta^{18}O_{carb}$ values agree well with those reported here. In general, geochemical data group according to phase type (body, fringe, spar), and some general trends characterize all of the concretions. All of the geochemical data reported here and previously are provided in Table 1.

British Concretions.—Both the body and fringe $\delta^{13}C_{carb}$ and $\delta^{18}O_{carb}$ values overlap and range from −18.3 to −8.6‰ and 0.0 to −2.7‰, respectively. Spar $\delta^{13}C_{carb}$ range from −2.9 to +1.3‰ and $\delta^{18}O_{carb}$ values range from −14.9 to −5.6‰. As can be seen in Figure 5, these data are very similar to those reported by previous investigators (Hudson 1978; Astin and Scotchman 1988; Martill and Hudson 1989; Hudson et al. 2001). Body and fringe clumped-isotope temperature values overlap somewhat, but body cements occupy a significantly larger range and include temperatures from 22 to 46°C. Fringe temperatures of precipitation cluster tightly and extend from 40 to 41°C. Body and fringe cements occupy a similar range in reconstructed $\delta^{18}O_{fluid}$ values, with all data ranging from +1.7 to +4.4‰. Spar temperatures and calculated $\delta^{18}O_{fluid}$ values extend from ~ 21 to 48°C and from −13.4 to 1.0‰, respectively. One bivalve shell from the Oxford concretion yields $\delta^{13}C_{carb}$ and $\delta^{18}O_{carb}$ values of +2.8 and −2.9‰, respectively. The clumped-isotope temperature and reconstructed $\delta^{18}O_{fluid}$ value are 45°C and +3.2‰, respectively (the high temperature of the bivalve shell reflects recrystallization, rather than a primary signal).

Moeraki Formation Concretion.—As with the British concretions, the concretion from the Moeraki Formation exhibits $\delta^{13}C_{carb}$ and $\delta^{18}O_{carb}$ values that overlap with those previously reported (Thyne and Boles 1989). New data on body and fringe cements cluster fairly tightly and exhibit $\delta^{13}C_{carb}$ and $\delta^{18}O_{carb}$ values that range from −20.0 to −16.4‰ and −4.1 to −2.8‰, respectively. The dark brown fringe sample plots closer to the body samples in $\delta^{13}C_{carb}$–$\delta^{18}O_{carb}$ space, largely due to a more depleted $\delta^{13}C_{carb}$ signature compared to the lighter, yellow-colored fringe. The spar cement exhibits a higher $\delta^{13}C_{carb}$ and a lower $\delta^{18}O_{carb}$ value compared to body and fringe phases (spar $\delta^{13}C_{carb}$ = −12.9‰, $\delta^{18}O_{carb}$ = −7.5‰).

The body cements in the Moeraki septarian concretion yield significantly cooler temperatures compared to the fringe and spar phases. Body precipitation temperatures and reconstructed $\delta^{18}O_{fluid}$ values range from 27 to 36°C and −0.4 to +1.5‰, respectively. The sampled spar produces a clumped-isotope temperature of 42°C and a reconstructed $\delta^{18}O_{fluid}$ of −1.9‰.

DISCUSSION

General Trends

For the most part, concretion bodies produce the lowest $\delta^{13}C_{carb}$ values, consistent with a significant organic-matter or methane source of carbon. Fringe cements can also exhibit quite low $\delta^{13}C_{carb}$ values (but not always) and when all of the data are considered together, spar phases yield the highest carbon isotope compositions. The transition to higher carbon isotope values in spar phases likely reflects a shift in carbon sources from dominantly organic (or methanic) to a more neutral marine (sourced from marine dissolved inorganic carbon or carbon derived from the dissolution of primary marine carbonate minerals) or methanogenesis-zone-derived dissolved inorganic carbon (Claypool and Kaplan 1974; Irwin et al. 1977; Raiswell and Fisher 2000). It is impossible to distinguish between these two heavy end members at this point because concretion $\delta^{13}C_{carb}$ values never exceed contemporaneous seawater carbon isotope compositions (Veizer et al. 1999; Zachos et al. 2001), which would indicate a methanogenesis-zone origin (Claypool and Kaplan 1974).

Carbonate oxygen isotope compositions tend to decrease from body to fringe to spar phases, and body and fringe cements group much more closely relative to spars. This progressive decrease in $\delta^{18}O_{carb}$ is generally thought to result from either burial-induced temperature increase (which yields a decreased fluid–rock oxygen isotope fractionation; Urey 1947; Kim and O'Neil 1997) or increased influence of meteoric-derived fluids. Whereas many processes can lead to a depletion in pore-water ^{18}O (Perry et al. 1976; Lawrence et al. 1979; Lawrence and Gieskes 1981; Marshall 1982; Sass et al. 1991), meteoric influx is the most commonly invoked because these fluids can deliver relatively large amounts of ^{16}O to marine pore waters (Gross 1964; Allan and Mathews 1982; Lohmann 1988). Distinguishing between meteoric influx and temperature increase with burial is a classic issue (see discussion in Mozley and Burns 1993) in carbonate-isotope interpretations in concretions and one that can be overcome by the use of clumped isotopes.

In general, concretion body, fringe, and spar phases express a systematic trend in precipitation temperatures (Figs. 5, 6). This recurring trend may support a progressive paragenetic evolution beginning with body cements precipitated at moderate temperatures, followed by fringe cements crystallized at slightly to somewhat elevated temperatures, and finally fringe-like to somewhat cooler spar formation conditions. Reconstructed $\delta^{18}O_{fluid}$ data suggest that a general decrease in water oxygen isotope compositions also occurred during progressive paragenetic (cement) evolution. The overall trends are consistent with initial heating followed by cooling and influence by meteoric fluids during the evolution of septarian concretions. Detailed interpretations of the British and Moeraki concretions are discussed below. Clumped-isotope-derived precipitation temperatures do not exceed maximum burial temperatures derived from independent means (see Fig. 5) (Thyne and Boles 1989;

←

FIG. 3.—Photomicrographs of septarian phases. **A)** Plain-polarized-light and **B)** cross-polarized-light images of a Kimmeridge Clay concretion. **C)** Close-up of fringe cement of a Kimmeridge Clay concretion, exhibiting bladed morphology. **D)** Cross-polarized image of a Kimmeridge Clay concretion. **E)** Plain-polarized and **F)** cross-polarized image of the Moeraki Formation concretion. **G)** Plain and **H)** cross-polarized image of a thin vein in the Moeraki Formation concretion. In images lt fringe, light fringe; dk fringe, dark fringe.

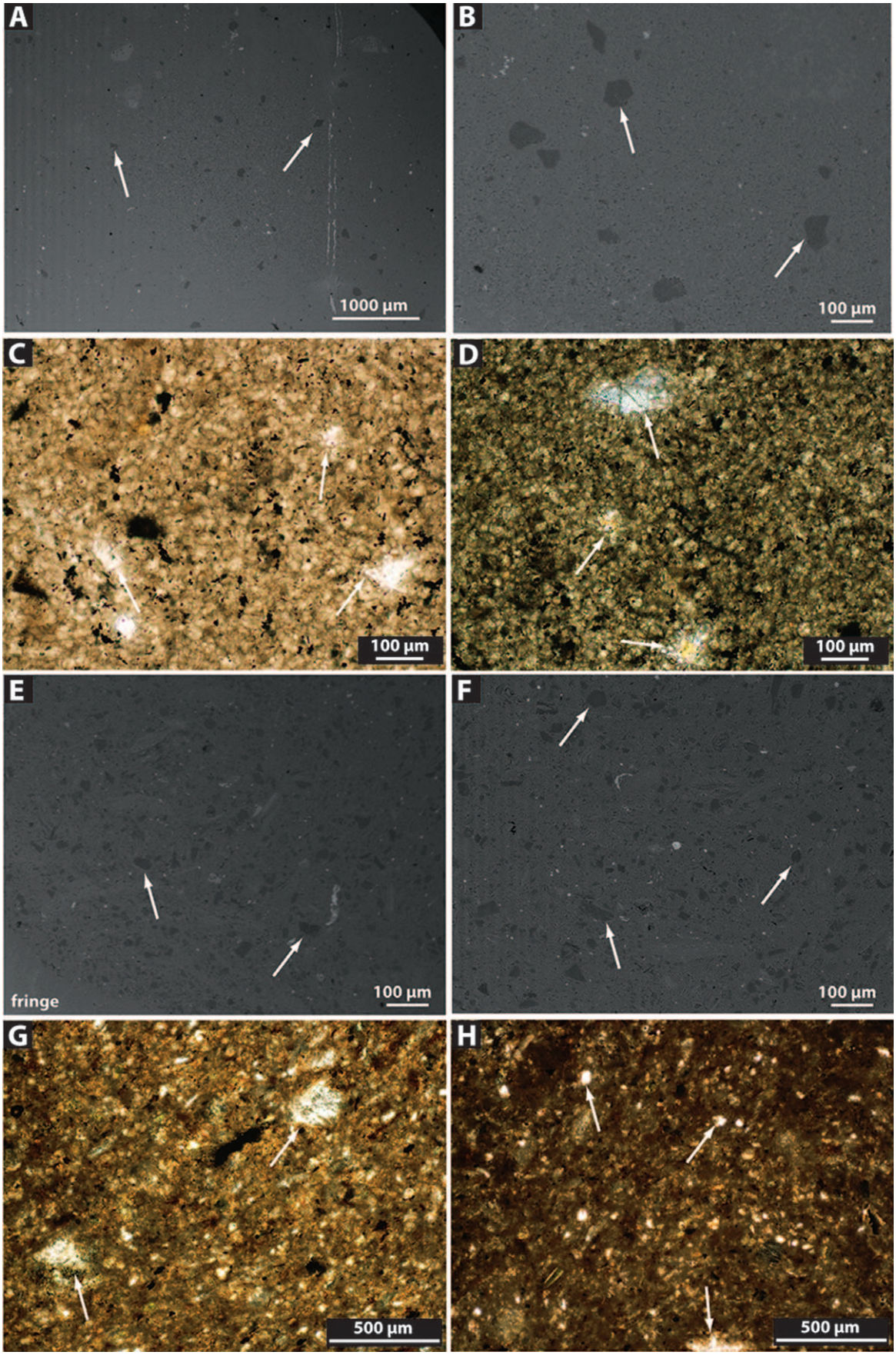
A
1000 µm
B
100 µm
C
100 µm
D
100 µm
E
fringe
100 µm
F
100 µm
G
500 µm
H
500 µm

Scotchman 1991). Figure 7 displays the interpreted paragenetic sequences graphically.

High Concretion Body Temperatures

Many concretions, both "normal" and septarian, exhibit textural characteristics that are consistent with formation at shallow depths. Evidence for shallow formation include external laminae deflection, high minus-cement porosities, the protection of delicate shells and otherwise primary depositional features in concretions, the preservation of magnetic mineral orientations (Wynne et al. 1995; Haggart et al. 2009), the recovery of nodules in relatively shallow (< 600 meters below seafloor) drill cores, and limited-depth reconstructed burial histories for the host unit. Maximum burial depths have been quantified for the British (Hudson 1978) and Moeraki (Boles et al. 1985) concretions examined here. Some of the British concretions contain uncrushed ammonites, well preserved microfossils, and minus-cement porosities up to ~ 95% by volume (Hudson 1978). These data suggest formation at relatively shallow sediment depths, which implies low temperatures. The British and Moeraki concretions exhibit body temperatures up to 46°C and 36°C, respectively, and are potentially unrealistically high when the shallow formation indices are considered. These high temperatures likely reflect multiple precipitation events in the concretion bodies, one of which occurred at relatively high temperature. Indeed, petrographic and backscatter SEM microscopy reveals two distinct carbonate phases in concretion bodies (Fig. 4). The coarse-crystalline pseudospar patches exhibit relatively high, third-order interference colors, indicative of calcite and not detrital silicate phases. The similar size and morphology of the electron dark phases and psuedospar patches suggests that they are the same. Opaque phases do occur throughout concretion bodies, but these are much larger and tend to exhibit irregular morphologies (Fig. 4). Therefore, we suggest that this secondary, calcite psuedospar phase precipitated at a higher temperature and recrystallized portions of the initial micritic body phase.

This style of complex paragenesis is similar to the pervasive style outlined by Raiswell and Fisher (2000) in that body cements did not form outward from a core or inward from a rim, but throughout the concretion interior with time (as first described by Mozley 1989). However, the straight-edged nature of the discrete phases (see Fig. 4) and the tendency for them to float within the surrounding body suggest that the later episodes of precipitation involved the *in situ* replacement of a precursory phase (replacement recognized in even very early studies, e.g., Clifton 1957).

The relationship between this recrystallization body phase and the fringe cements is unclear at this point. However, comparison of fringe and body temperature and $\delta^{18}O_{fluid}$ data provides evidence in support of contemporary emplacement of the fringes and the body recrystallization phases. Fringe phases tend to exhibit the highest temperatures and $\delta^{18}O_{fluid}$ values, and body phases express positively correlated trends toward the fringe end member (Figs. 5, 6). If extrapolated linearly, these arrays extend toward a potential lower end-member with temperature–$\delta^{18}O_{fluid}$ values much closer to shallow marine pore waters (~ 15–20°C and $\delta^{18}O_{fluid}$ ~ −2 to 0‰). Therefore concretion bulk bodies may represent a mixture of two end member phases, a cool and low $\delta^{18}O_{fluid}$ marine end member and a hot and high $\delta^{18}O_{fluid}$ end member.

British Concretions: Comparisons with Previous Works

Previous investigators extensively examined concretions from the Kimmeridge, Ampthill, and Oxford Clays (see Hudson 1978; Astin and Scotchman 1988; Scotchman 1991; Hudson et al. 2001) and proposed more or less similar paragenetic interpretations regarding cement precipitation environments. One predominant difference corresponds to a combined temperature plus meteoric influx–induced (Astin and Scotchman 1988; Scotchman 1991) rather than strictly meteoric influx–derived (Hudson 1978; Hudson et al. 2001) depletion in $\delta^{18}O_{carb}$ of spar cements. The two different interpretations are based on previous analyses of Kimmeridge concretions (Astin and Scotchman 1988; Scotchman 1991) and Ampthill and Oxford concretions (Hudson 1978; Hudson et al. 2001). Intriguingly, clumped-isotope and reconstructed $\delta^{18}O_{fluid}$ values for these septarian concretions plot similarly (see Fig. 5), and the trends among phases are identical. Unlike traditional $\delta^{18}O_{carb}$ values, which are ambiguous with regard to a temperature versus meteoric derived signal, clumped-isotope compositions can yield an independent constraint on temperature. New data suggest a similar origin for all of the cement phases of the British septarian concretions and support an interpretation similar to that of Scotchman (1991), as discussed in detail below.

Concretion bodies in these concretions have been interpreted as forming early, in relatively shallow sediments experiencing sulfate reduction. A sulfate-reduction-zone origin is supported by depleted $\delta^{13}C_{carb}$ values, low carbonate-bound iron contents and the presence of pyrite in the concretions (Hudson 1978; Astin and Scotchman 1988; Scotchman 1991; Hudson et al. 2001; this study). High organic-carbon contents of the hosts suggest that these marine sediments would have been prone to extensive sulfate reduction (Jorgensen 1977). Precipitation in proximity to the sediment–water interface is supported by the physical attributes discussed above as well as $\delta^{18}O_{carb}$, reconstructed $\delta^{18}O_{fluid}$, and strontium isotope compositions that are similar to (Sr isotope compositions slightly elevated in Oxford and Ampthill concretions) contemporaneous seawater (Scotchman 1991; Hudson et al. 2001).

The fringe cements exhibit $\delta^{13}C_{carb}$ and $\delta^{18}O_{carb}$ values similar to those of the concretion bodies (although some display compositions markedly enriched in ^{13}C), supporting a shallow formation depth like that invoked for the body cements. However, Hudson et al. (2001) note that the fringe cement exhibits highly variable iron contents, interpreted to represent input from iron oxide reduction-derived pore-water Fe. These fringe calcites also exhibit the most seawater-like Sr-isotope compositions.

Spar calcites yield heavier $\delta^{13}C_{carb}$ and lighter $\delta^{18}O_{carb}$ compared to the fringe and body cements. The spars also exhibit strontium isotope compositions that are significantly more radiogenic than contemporaneous seawater (Oxford and Ampthill only; Kimmeridge Sr isotope compositions were not measured) and relatively high iron contents (Scotchman 1991; Hudson et al. 2001). Hudson et al. (2001) also note that both iron and strontium show a "crude" negative correlation with $\delta^{18}O_{carb}$. All of these data suggest a precipitation environment significantly removed from a marine setting (or early diagenetic setting). Both Scotchman (1991) and Hudson et al. (2001) interpret these trends as reflective of spar precipitation in the presence of meteoric-derived fluids, although the former also suggests precipitation at somewhat elevated temperatures as well.

The spar data presented here are not at complete odds with the interpretations of Hudson et al. (2001), but rather reflect a general

←

FIG. 4.—Plain-polarized-light, cross-polarized-light, and electron-backscatter SEM images of **A–D)** British and **E–F)** Moeraki septarian concretions. Arrows in BSE images (A, B, E, F) identify an electron dark phase that occurs in all concretions analyzed. The dark phase is straight-edged and "floats" in electron light phase. Arrows in plain-polarized and cross-polarized micrographs (C, D, G, H) identify similar-sized, straight-edged patches of coarse-crystalline carbonate. As can be seen in Part D, these patches exhibit the third-order interference colors typical of carbonate minerals. Opaque materials in Parts C and G generally exhibit much more irregular morphology, in contrast to the electron dark phases.

TABLE. 1.—*Geochemical data including stable-isotope and clumped-isotope compositions. Samples are listed by locality and phase.*

Sample		$\delta^{13}C_{carb}$	$\delta^{13}C_{carb}$	$\delta^{18}O_{carb}$	$\delta^{18}O_{carb}$	Δ_{47}	Δ_{47}	Temp.	Temp	$\delta^{18}O_{fluid}$	$\delta^{18}O_{fluid}$
ID	Cement Type	(‰, PDB)	St Dev	(‰, PDB)	St Dev	(‰)	St Err	(°C)	St Err	(‰, SMOW)	(‰)
MOERAKI CONCRETION											
this study											
B1-H1	Body	−20.95	0.01	−2.96	0.02	0.663	0.005	35	1	1.5	0.2
B1-H2	Body	−19.26	0.00	−3.19	0.02	0.702	0.011	27	2	−0.4	0.5
B1-F2	Dark Fringe (early)	−19.41	0.00	−3.05	0.01	0.622	0.014	45	4	3.2	0.6
B1-F3	Light Fringe (later)	−16.76	0.01	−2.84	0.01	0.623	0.007	45	2	3.4	0.3
B1-F1	Light Fringe (later)	−16.41	0.00	−3.14	0.01	0.635	0.012	42	3	2.6	0.5
B1-F4	Light Fringe (later)	−16.48	0.01	−4.08	0.02	0.623	0.014	45	3	2.1	0.6
B1-SS	Spar	−12.89	0.01	−7.48	0.01	0.612	0.012	42	3	−1.9	0.5
Previously Reported (Thyne and Boles 1989)											
NZ1-CB	Body	−15.20		−2.00							
NZ1-CB2	Body	−30.30		−2.00							
NZ2-CB	Body	−19.80		−1.61							
NZ2-CB2	Body	−20.10		−1.61							
NZ2-CB3	Body	−27.40		−1.71							
NZ2-CB4	Body	−30.80		−1.42							
NZ1-EBC	Dark Fringe	−29.50		−1.42							
NZ2-EBC	Dark Fringe	−29.50		−2.00							
NZ2-EBC2	Dark Fringe	−28.70		−1.32							
NZ2-EBC3	Dark Fringe	−29.70		−1.71							
NZ3-EBC	Dark Fringe	−23.70		−1.81							
NZ2-Inner 'spar'	Light Fringe	−18.20		−6.08							
NZ2-Inner 'spar' 2	Light Fringe	−18.30		−5.49							
NZ2-Inner 'spar' 3	Light Fringe	−18.20		−5.59							
NZ2-Outer Spar	Spar	−11.10		−8.99							
NZ2-Outer Spar 2	Spar	−13.10		−8.02							
NZ2-Outer Spar 3	Spar	−18.20		−6.66							
NZ1-Outer Spar	Spar	−11.20		−8.99							
NZ3-Outer Spar	Spar	−15.70		−7.34							
BRITISH CONCRETIONS											
Ampthill											
this study											
jad-sc-1	Body	−16.87	0.02	−2.66	0.03	0.642	0.010	41	2	2.7	0.5
jad-sc-2	Body	−17.50	0.02	−2.36	0.04	0.621	0.005	46	1	4.0	0.2
jad-sc-3	Fringe	−19.27	0.01	−1.29	0.02	0.639	0.011	41	3	4.2	0.5
jad-sc-5	Spar	−2.71	0.01	−10.53	0.03	0.650	0.013	38	3	−5.6	0.6
Ampt Spar	Spar	−2.92	0.02	−9.92	0.05	0.612	0.009	48	2	−3.2	0.4
P3-4r	Spar	1.33	0.02	−7.64	0.02	0.681	0.009	32	2	−4.0	0.4
Previously Reported (Hudson 2001)											
P3-1	body	−19.34		−0.24							
P3-2	body	−18.91		−0.91							
P5953A	Fringe	−13.04		−0.90							
P3-3	fringe	−17.03		−0.83							
P3-4	spar	−3.00		−9.33							
P5951A	Spar	−3.11		−9.36							
Kimmeridge											
this study											
TS-H1	Body	−8.58	0.00	−0.01	0.01	0.728	0.011	22	2	1.7	0.5
TS-H2	Body	−15.23	0.00	−1.95	0.01	0.644	0.006	40	2	3.3	0.3
TS-F2	Fringe	−15.54	0.00	−2.61	0.01	0.643	0.010	40	2	2.7	0.4
TS-S1	Spar	0.45	0.00	−5.64	0.02	0.636	0.010	42	2	0.0	0.4
TS-S2	Spar	−1.83	0.01	−5.90	0.02	0.549	0.007	49	2	1.0	0.3
TS-S3	Spar	0.25	0.00	−14.89	0.02	0.732	0.008	21	2	−13.4	0.3
Oxford											
this study											
OxB1	Body	−14.47	0.03	−0.73	0.03	0.673	0.009	33	2	3.3	0.4
OxF1	Fringe	−14.04	0.02	−0.98	0.01	0.643	0.016	40	4	4.4	0.7
P5-2	Spar	−0.48	0.02	−7.31	0.01	0.645	0.012	40	3	−2.1	0.5
Shell	Shell in concretion	2.85	0.01	−2.95	0.01	0.626	0.012	45	3	3.2	0.5
Previously Reported (Hudson 1978)											
C1A-1	Body	−11.98		−0.82							
C1C1A	Body	−11.98		−0.60							
C1C2A	Fringe	−8.83		−2.14							
C1C2A-d	Fringe	−8.67		−2.48							
C1B-1	Fringe	−12.76		−0.48							

TABLE 1.—*Continued.*

Sample ID	Cement Type	$\delta^{13}C_{carb}$ (‰, PDB)	$\delta^{13}C_{carb}$ St Dev	$\delta^{18}O_{carb}$ (‰, PDB)	$\delta^{18}O_{carb}$ St Dev	Δ_{47} (‰)	Δ_{47} St Err	Temp. (°C)	Temp St Err	$\delta^{18}O_{fluid}$ (‰, SMOW)	$\delta^{18}O_{fluid}$ (‰)
C1B-2	Spar	−7.28		−3.61							
P5-2	Spar	−3.28		−9.30							
C1C3A	Spar	−7.17		−3.59							
C1C3B	Spar	−0.54		−5.35							

agreement. In fact the reconstructed $\delta^{18}O_{fluid}$ values extending down to ~ -6‰ agree well with the ~ -7‰ value reported for Late Jurassic rainwater of the area (Marshall and Ashton 1980). In addition, the spread in $\delta^{13}C_{carb}$ and $\delta^{18}O_{carb}$ interpreted to represent regional variation in hydrology mimics the large ranges in clumped-isotope temperatures and $\delta^{18}O_{fluid}$, indicating variability in multiple thermochemical parameters. However, the new clumped-isotope data suggest that temperatures were somewhat elevated, which we interpret as reflecting a meteoric-derived fluid that was subsequently heated before spar precipitation, similar to the interpretations for Kimmeridge concretions derived by Scotchman (1991). The possibility of significantly elevated fluid temperatures was discounted by previous workers (Hudson 1978; Hudson et al. 2001) based largely on the presence of preserved biomarkers (Hudson and Martill 1994). However, the 50°C maximum burial temperature dictated by these biomarkers is not exceeded by any of the British clumped-isotope-derived temperatures presented here (see Fig. 5). Incidentally a similar lower maximum burial temperature has been developed for the Kimmeridge Clay (Ebukanson and Kinghorn 1985, 1986; Penn et al. 1986; Sellwood et al. 1989; McLimans and Videtich 1989; Green 1989a, 1989b; Scotchman 1991).

The variable iron contents in the fringe cements may indicate inputs from distinct fluids rather than fluctuating redox horizons (as was interpreted by Hudson et al. 2001). Dissolved-iron contents can be variably elevated in deeper pore waters, and elevated iron contents have been recorded in concretions that formed at depths below the iron reduction zone (Scotchman 1991; Loyd et al. 2012b). A somewhat deeper fringe-precipitation environment therefore satisfies both the iron concentrations and the elevated temperatures derived from clumped-isotope analyses. In addition, the elevated reconstructed $\delta^{18}O_{fluid}$ values agree with a somewhat deeper formation environment because water–rock interactions (which tend to be more significant at depth) can introduce a preferential amount of ^{18}O to pore waters (Clayton et al. 1966; Morton and Land 1987; Banner and Hanson 1990).

We now construct a revised paragenetic evolution that draws from all of the data available for the studied British concretions. The similarity in the data has prompted us to consider a more or less similar paragenesis for all of the septarian concretions from this general locality. Initially, the body phase precipitated in shallow sediments potentially within the lower sulfate reduction zone (a zone conducive to carbonate-mineral precipitation; Raiswell and Fisher 2000) as hypothesized by Hudson (1978) and Astin and Scotchman (1988). The shallow pore fluids participating in precipitation were very similar to contemporaneous marine fluids with neutral $\delta^{18}O_{fluid}$, elevated strontium contents, low iron contents, and near seawater strontium isotope compositions. The septarian cracking must have occurred after body formation but before fringe cementation. After cracking and some burial, fringe cements precipitated with variable and elevated iron contents and elevated $\delta^{18}O_{fluid}$ compositions. The sea-water strontium isotope composition can be preserved as long as no diagenetic process is acting to significantly modify pore-water $^{87/86}Sr$, diffusive transport of Sr does not significantly alter its isotope composition (Palmer and Elderfield 1985), and/or if the strontium is being derived from primary marine carbonate dissolution. Finally, heated meteoric fluids penetrated the host unit and led to the precipitation of spar cements. The transition from a dominantly buried seawater to a meteoric-derived source fluid agrees well with the distinct geochemistry of the spar phases compared to the fringe and body phases. The positive correlation between clumped-isotope temperatures and $\delta^{18}O_{fluid}$ values in spar cements (Figs. 5, 6) suggests that spar precipitation began at near maximum depth and continued throughout subsequent uplift, reflected by a trend towards cooler temperatures and a more significant meteoric component (more depleted in ^{18}O). The emplacement of the replacing body phase is less straightforward, but the absence of an electron-dark phase within fringe and spar phases suggests precipitation prior to fringe formation. The fact that the fringe cements exhibit temperatures higher than the overall body temperatures may indicate that the replacement body and fringe phases were emplaced simultaneously. One distinct difference between the Kimmeridge and Oxford and Ampthill concretions is strontium concentrations in the spar phases. Whereas Sr contents are relatively low in the latter, Kimmeridge concretions show a relative increase in the spar phases. This is thought to reflect an increase in strontium derived from the dissolution of primary carbonate minerals (aragonite fossils and/or coccoliths) (Scotchman 1984, 1989, 1991). Regardless of this slight difference, all of the British concretions show strikingly similar geochemical, and by extension, paragenetic evolutionary, histories.

Moeraki Concretion: Comparisons with Previous Works

Moeraki Formation septarian concretions similar to the one analyzed here were studied by Boles et al. (1985) and Thyne and Boles (1989). This earlier work provides additional petrographic and geochemical information that the new clumped-isotope data complement. Intriguingly, the Moeraki concretions exhibit petrographic and geochemical characteristics that mimic those observed in the British septarian concretions discussed above.

The concretion body cements analyzed here and by previous investigations yield $\delta^{13}C_{carb}$ and $\delta^{18}O_{carb}$ values consistent with early formation in shallow sediments undergoing sulfate reduction. The occurrence of organic matter and framboidal pyrite (Fig. 4) in concretion bodies provides additional evidence that sulfate reduction likely operated during the early stage of concretion precipitation (Boles et al. 1985; this study). An additional input of methane-derived carbon is evident in some, but not all, samples (Thyne and Boles 1989). In addition, microprobe analyses indicate relatively low iron and manganese contents in body cements (Boles et al. 1985). The relatively low clumped-isotope temperatures (note that body phases are skewed toward somewhat higher temperatures as discussed above) and neutral reconstructed $\delta^{18}O_{fluid}$ values are consistent with the shallow precipitation environment interpreted by Boles et al. (1985) and Thyne and Boles (1989).

Fringe cements exhibit relatively elevated $\delta^{13}C_{carb}$, $\delta^{18}O_{carb}$, clumped isotope temperatures, and $\delta^{18}O_{fluid}$ values, whereas elemental concentrations coincide with those exhibited by the body cements. The brown and yellow fringes display overlapping geochemical values, indicating that the two fringes formed under similar conditions. The Moeraki fringe phases likely formed at somewhat deeper burial depths in pore waters with elevated $\delta^{18}O$ sourced from water–rock interactions, just as in the British fringe cements. However, the Moeraki fringes seem to have formed in

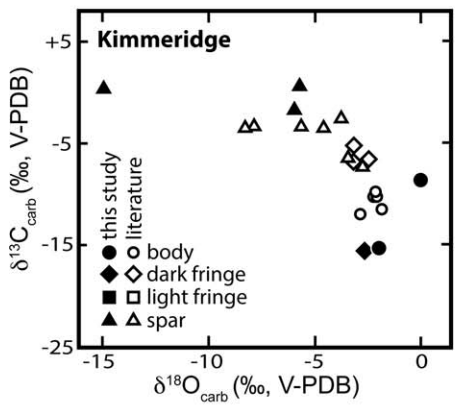
Kimmeridge
this study
literature
body
dark fringe
light fringe
spar
δ13Ccarb (‰, V-PDB)
δ18Ocarb (‰, V-PDB)

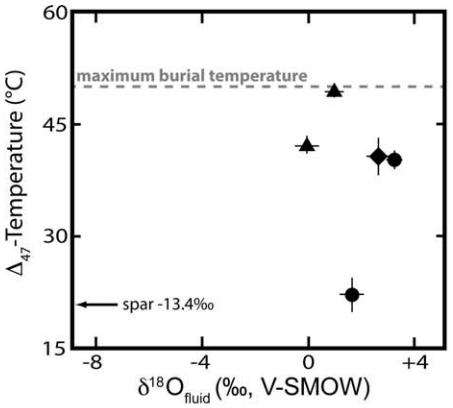
maximum burial temperature
spar -13.4‰
Δ47-Temperature (°C)
δ18Ofluid (‰, V-SMOW)

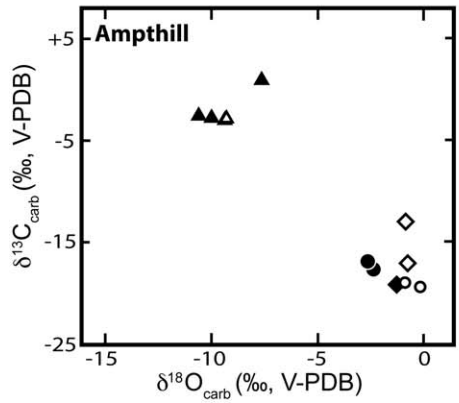
Ampthill
δ13Ccarb (‰, V-PDB)
δ18Ocarb (‰, V-PDB)

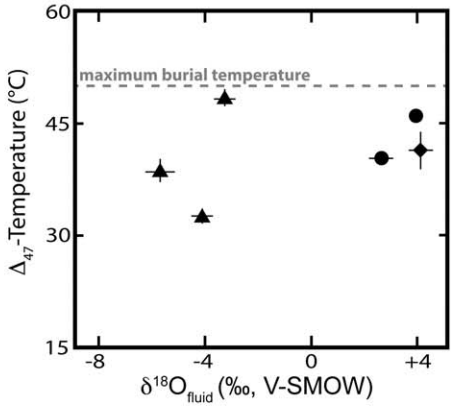
maximum burial temperature
Δ47-Temperature (°C)
δ18Ofluid (‰, V-SMOW)

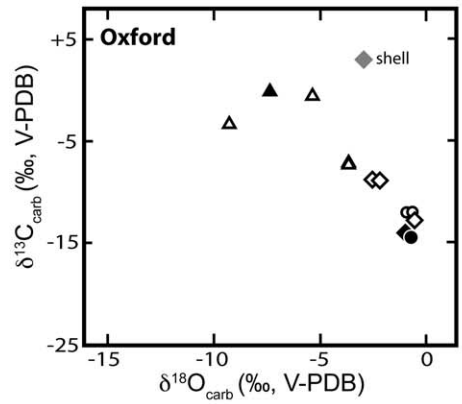
Oxford
shell
δ13Ccarb (‰, V-PDB)
δ18Ocarb (‰, V-PDB)

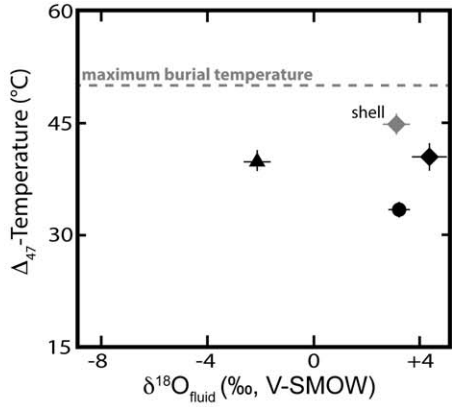
maximum burial temperature
shell
Δ47-Temperature (°C)
δ18Ofluid (‰, V-SMOW)

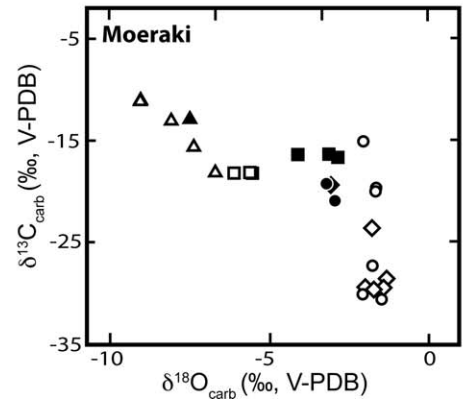
Moeraki
δ13Ccarb (‰, V-PDB)
δ18Ocarb (‰, V-PDB)

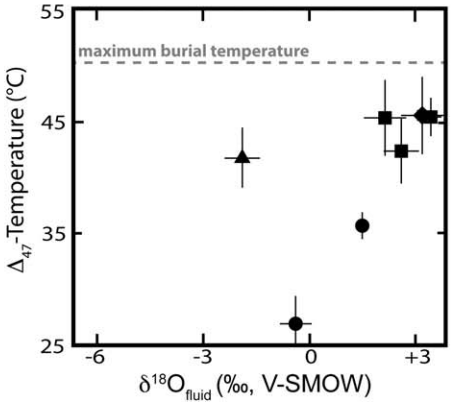
maximum burial temperature
Δ47-Temperature (°C)
δ18Ofluid (‰, V-SMOW)

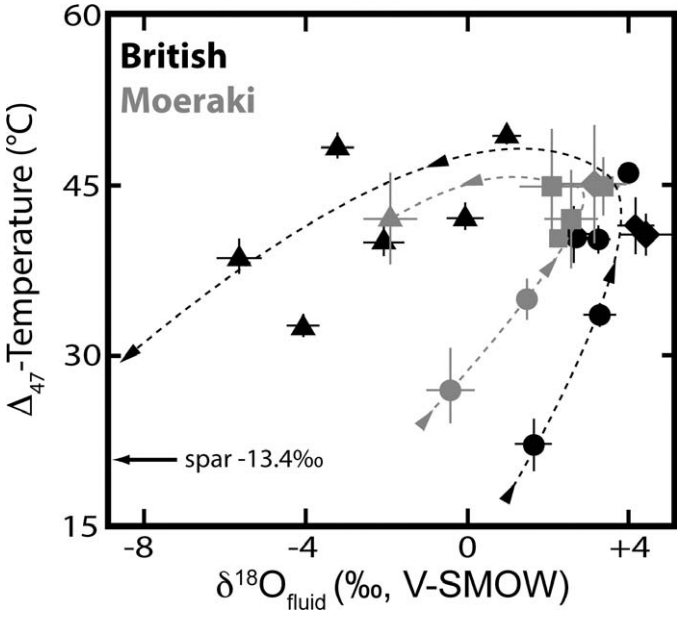

FIG. 6.—Compiled temperature and $\delta^{18}O_{fluid}$ data. The arrowed dashed lines reflect the paragenetic evolution as supported by trends in successive septarian phases. Notice how the general trend is similar among British and Moeraki concretions. Phase labeling is the same as in Figure 5.

pore waters receiving a more substantial input of organic matter-derived (or methane-derived) carbon (compare $\delta^{13}C_{carb}$ values in Fig. 5). The relatively low iron contents in the fringe phases analyzed by Boles et al. (1985) suggest that although formed deeper than body phases, the fringes formed mainly in sediments with a significant non-carbonate iron sink, such as pyrite forming in the sulfate-reduction zone. Thyne and Boles (1989) interpret the body and fringe cements as having formed contemporaneously; this agrees well with our interpretation that a secondary body phase was emplaced contemporaneously with fringes.

The spar cements of the Moeraki concretions analyzed here and elsewhere exhibit geochemical characteristics that are wholly distinct from the fringe and body phases. The spars exhibit elevated iron contents, manganese contents, and $\delta^{13}C_{carb}$ values and depleted $\delta^{18}O_{carb}$ and reconstructed $\delta^{18}O_{fluid}$ values (Boles et al. 1985; Thyne and Boles; 1989; this study). The single clumped isotope temperature of the spar cement overlaps with the fringe cements, suggesting that spar formed at similar temperatures and by extension similar depths as the fringe phases. However, the fluids involved in spar precipitation must have been otherwise very different from those that produce the fringe and concretion body phases. As with the British concretions, the geochemical data as a whole indicate spar formation from a fluid that exhibited a significant meteoric component, consistent with interpretations by Thyne and Boles (1989). The reconstructed $\delta^{18}O_{fluid}$ values calculated here are slightly elevated compared to the ~ -8 to -5‰ values predicted by Thyne and Boles (1989), but this likely arises due to uncertainties in the end-member meteoric $\delta^{18}O_{fluid}$ value and mixing ratios between fluids. Ultimately, the data as a whole are consistent with the same mixed-meteoric-fluid interpretation.

The maximum host unit temperatures of $\sim$ 50°C revealed by vitrinite reflectance data (Boles et al. 1985) exceed the clumped-isotope temperatures reported here. The geochemical trends among phases indicate a diagenetic progression similar to that derived for the British concretions. Body cements initially formed in the sulfate reduction zone that may have received some upwardly diffusing carbon sourced from methane. The fringe phases precipitated after septarian cracking in somewhat deeper sediments with pore waters elevated in ^{18}O. Subsequently, and potentially after a significant amount of time, spar phases were precipitated from reducing, mixed-meteoric fluids. With only a single spar clumped-isotope analysis, it is difficult to assess whether or not this late septarian phase precipitated during uplift of the host unit (as supported by a positive correlation between temperature and $\delta^{18}O_{fluid}$ in the British concretions).

Implications for Formation Models of Septarian Concretions

Interestingly, the septarian concretions analyzed here exhibit similar overall trends in geochemical data even though each are derived from disparate host units of differing ages and depositional environments. The similarities suggest that these septarian concretions experienced similar paragenetic evolutions. Whereas the mechanism(s) of septarian cracking cannot be identified with the data presented here, it seems intriguing that cement paragenesis across chemically dynamic regimes was occurring potentially contemporaneously with septarian cracking. Aside from this intriguing yet convoluted issue, two overarching trends deserve additional discussion; these include progressive enrichment in $\delta^{13}C_{carb}$ and depletion in $\delta^{18}O_{fluid}$ in subsequent septarian cement phases.

Progressive Enrichment in $^{13}C_{carb}$ and Partial Early Diagenetic Precipitation.—Unlike oxygen isotope compositions in carbonate systems, very little carbon isotope fractionation accompanies the conversion from aqueous carbon (dissolved inorganic carbon: DIC) to solid-phase carbonates. Likewise, oxidation of organic carbon and methane are not accompanied by a significant fractionation. Therefore, $\delta^{13}C_{carb}$ is traditionally used as a direct proxy for $\delta^{13}C_{DIC}$ and by extension represents a straightforward tracer for the precursor carbon source (e.g., methane, organic carbon, seawater DIC, etc.) (e.g., Irwin et al. 1977). In addition, temperature does not strongly influence carbon isotope fractionation during the precipitation of carbonate minerals (Clark and Fritz 1997, p. 30), therefore securing its utility as a relatively clear-cut tracer.

The spread in $\delta^{13}C_{carb}$ values among septarian phases reflects the high variability in $\delta^{13}C_{DIC}$ exhibited in diagenetic systems. These variations are largely dictated by differential influences by organo-diagenetic processes that occur in shallow marine sediments. These processes include organic-matter oxidation and/or methane oxidation or production and can increase or decrease the ambient pore-water $\delta^{13}C_{DIC}$. Indeed, with progressive burial (within "shallow" sediments) pore waters tend to exhibit an initial trend from neutral $\delta^{13}C_{DIC}$ values (reflecting overlying sea-water $\delta^{13}C$ values) to negative $\delta^{13}C_{DIC}$, indicating an input from carbon derived organic-matter or methane. With deeper burial, this trend may reverse and pore waters may exhibit an increase in $\delta^{13}C_{DIC}$ reflecting the process of methanogenesis (Claypool and Kaplan 1974). With even deeper burial, the trend may reverse once more as sediments are exposed to higher temperatures and as a result residual organic carbon is degraded thermally.

The body cements of the septarian concretions analyzed here exhibit very low $\delta^{13}C_{carb}$ values, reflecting carbon derived from the remineralization of organic carbon and/or the oxidation of methane. These

←

FIG. 5.—Isotope cross plots for the concretions analyzed here and data reported in the literature. Left column corresponds to $\delta^{18}O_{carb}$–$\delta^{13}C_{carb}$ plots, and the right column corresponds to $\delta^{18}O_{fluid}$–temperature plots. Also plotted are the maximum burial temperatures as derived from independent means reported in the literature (see main text). Some previously reported data have been adapted from images and are not included in Table 1. These correspond to data reported in Astin and Scotchman (1988) and Scotchman (1991).

British Septarian Concretions

Body cement precipitation within sulfate-reduction zone in shallow sediments

Initial phase of **septarian cracking**

Fringe precipitation below the sulfate-reduction zone in sediments exhibiting temperatures ~ 40°C

Body recrystallization must have occured after initial body cementation and likely contemporaneously with fringe emplacement

Spar Precipitation during progressive uplift with increased exposure to meteoric fluids exhibiting $\delta^{18}O_{fluid}$ down to −6‰

Moeraki Septarian Concretion

Body cement precipitation within sulfate-reduction zone in shallow sediments that also experienced methane oxidation.

Septarian cracking

Fringe precipitation below the sulfate-reduction zone in deeper sediments exhibiting temperatures ~ 45°C, slightly elevated $\delta^{18}O_{fluid}$ and with a significant source of organic carbon- and/or methane-derived DIC

Body recrystallization must have occured after initial body cementation and likely contemporaneously with fringe emplacement

Spar Precipitation in fluids with low $\delta^{18}O_{fluid}$ potentially reflecting a significant meteoric component.

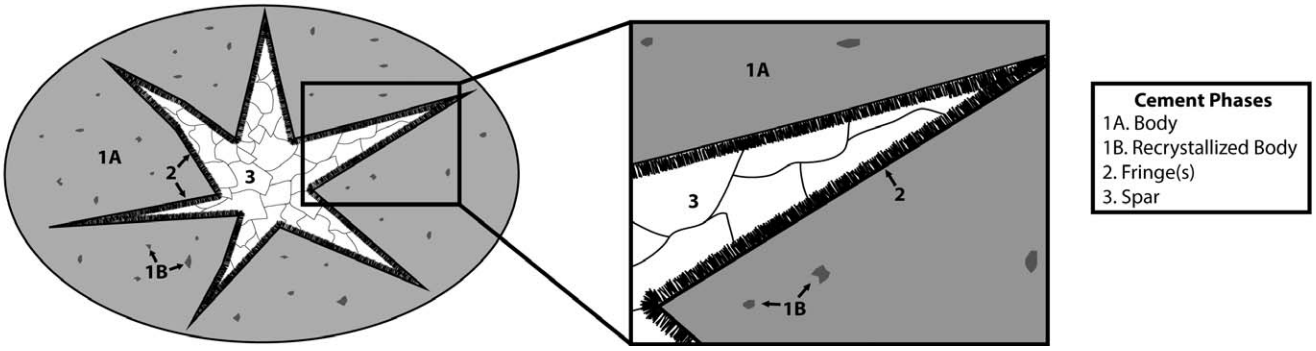

FIG. 7.—Paragenetic interpretation. The diagram generically depicts the cement phases.

processes are common in modern, shallow marine sediments that contain organic carbon. Therefore the concretion bodies of these concretions likely formed in a shallow diagenetic environment experiencing organo-diagenesis. Successive cement phases are progressively enriched in ^{13}C potentially reflective of two processes: 1) continued precipitation in somewhat deeper sediments experiencing methanogenesis or 2) precipitation outside of the organo-diagenetic realm.

The smooth trends reflected in $\delta^{18}O_{carb}$ -$\delta^{13}C_{carb}$ crossplots might be taken to indicate process 1 above, in as much as successive precipitation with burial is relatively easy to envision. However, the clumped-isotope data presented here indicate that process 2 is more likely and that the smooth trends in $\delta^{18}O_{carb}$ −$\delta^{13}C_{carb}$ space are the coincidental outcomes of very different formation environments.

Progressive Cooling, Depletion in $^{18}O_{fluid}$, and Meteoric-Fluid Involvement.—As can be seen in Figure 6, the depletion in spar $^{18}O_{carb}$ is the combined result of moderate temperatures and low $\delta^{18}O_{fluid}$ values. Where significant data have been collected (British concretions), increased temperatures generally coincide with increased $\delta^{18}O_{fluid}$ values. We suggest that the correlation reflects initial precipitation of spar phases at depth and continued precipitation within cooler fluids experiencing increasing contributions from a meteoric source. Indeed, previous investigators (Hudson 1978; Astin and Scotchman 1988; Scotchman 1991; Hudson et al. 2001) have suggested that precipitation of spar in similar British septarian concretions occurred in fluids with a significant meteoric component. Whereas the data presented here confirm these previous interpretations, they furthermore provide a more developed picture of paragenesis. The decrease in temperature and more meteoric-like $\delta^{18}O_{fluid}$ values are consistent with progressive spar precipitation during uplift. The data are insufficient for the Moeraki concretions to resolve a similar correlation; however, the position of the single spar data point is similar to spar data exhibited by the British concretions (see Fig. 6). Such late-stage, uplift-related spar precipitation has been proposed in non-concretionary carbonate units (Loyd et al. 2013). These new data suggest that uplift-related spar formation might be more common than previously thought and specifically related to spar precipitation in septarian concretions. These findings are quite different from those of Dale et al. (2014), who find that late-stage spars of the Mancos Shale septarian concretions exhibit relatively high temperatures and neutral $\delta^{18}O_{fluid}$ values, perhaps testament to the potential of variable septarian concretion formation environments.

CONCLUSIONS

As has been recognized previously, body, fringe, and spar cements of septarian concretions from four different host units of two different localities exhibit variable $\delta^{18}O_{carb}$ and $\delta^{13}C_{carb}$, suggestive of phase precipitation from distinct fluids. Clumped-isotope analyses reveal similarly variable precipitation temperatures and reconstructed $\delta^{18}O_{fluid}$ values, consistent with the complex parageneses suggested by the traditional isotopic analyses. Body cements formed at lower temperatures and from fluids with more neutral $\delta^{18}O_{fluid}$ values than fringe cements, which exhibit higher temperatures and enriched $\delta^{18}O_{fluid}$. This is consistent with sequential precipitation of the concretion body then fringe cements with burial in fluids that shift from unmodified buried seawater to those elevated in ^{18}O, potentially due to water–rock interactions at depth. Fringe emplacement may have coincided with the recrystallization of isolated portions of concretion bodies as reflected in bulk geochemical trends. The new $\delta^{18}O_{fluid}$ values presented here confirm the involvement of meteoric fluids in spar precipitation, as had been previously suggested for Moeraki and British septarian concretions. However, these spars also exhibit somewhat elevated precipitation temperatures that overlap with hotter fringe temperatures and correlate positively with $\delta^{18}O_{fluid}$ values in the British concretions. This suggests that the depleted $\delta^{18}O_{carb}$ values reflect both increased temperatures and

depleted $\delta^{18}O_{fluid}$ values and that spar precipitation began at depth and likely continued during uplift of the host units. During this uplift, decreasing distances from the surface facilitated increasing input of meteoric fluids. These and similar instances of uplift-related spar precipitation have been identified, suggesting that this style of cementation may be more widespread than previously thought.

SUPPLEMENTARY DATA

Supplemental Data Table 1 is available from JSR's Data Archive: http://sepm.org/pages.aspx?pageid=229.

ACKNOWLEDGMENTS

We would like to thank John Hudson for insightful discussions, and members of the Tripati Lab group and Rob Eagle for analytical assistance. The final manuscript benefitted from insightful reviews and comments by Jim Marshall, Reinhard Hesse, and Associate Editor Luis Fernando De Ros. Financial support provided by the Agouron Institute Postdoctoral Fellowship, American Chemical Society–Petroleum Research Fund grant 51182-DNI2, Department of Energy BES grant DE-FG02-13ER16402, National Science Foundation grants EAR-0949191 and ARC-1215551, and a Hellman Fellowship.

REFERENCES

Allan, J.R., and Mathews, R.K., 1982, Isotope signatures associated with early meteoric diagenesis: Sedimentology, v. 29, p. 797–817.

Astin, T.R., 1986, Septarian crack formation in carbonate concretions from shales and mudstones: Clays and Clay Minerals, v. 21, p. 617–631.

Astin, T.R., and Scotchman, I.C., 1988, The diagenetic history of some concretions from the Kimmeridge Clay, England: Sedimentology, v. 35, p. 349–368.

Banner, J.L., and Hanson, G.N., 1990, Calculation of simultaneous isotopic and trace element variations during water–rock interaction with application to carbonate diagenesis: Geochimica et Cosmochimica Acta, v. 54, p. 3123–3137.

Bathurst, R.G.C., 1975, Carbonate sediments and their diagenesis, Second Edition: Amsterdam, Elsevier, 620 p.

Berner, R.A., 1980, Early Diagenesis—A Theoretical Approach: Princeton, N.J., Princeton University Press, Princeton Series in Geochemistry, 241 p.

Boles, J.R., Landis, C.A. and Dale, P., 1985, The Moeraki Boulders: anatomy of some septarian concretions: Journal of Sedimentary Research, v. 55, p. 398–406.

Bristow, T.F., Bonifacie, M., Derkowski, A., Eiler, J.M., and Grotzinger, J.P., 2011, A hydrothermal origin for isotopically anomalous cap dolostone cements from south China: Nature, v. 474, p. 68–71.

Came, R.E., Eiler, J.M., Veizer, J., Azmy, K., Brand, U., and Weidman, C.R., 2007, Coupling of surface temperatures and atmospheric CO_2 concentrations during the Paleozoic Era: Nature, v. 449, p. 198–201.

Clark, I.D., and Fritz, P., 1997, Environmental Isotopes in Hydrogeology: New York, Lewis Publishers, CRC Press, 328 p.

Claypool, G.E., and Kaplan, I.R., 1974, The origin and distribution of methane in marine sediments, *in* Kaplan, I.R., ed., Natural Gases in Marine Sediments: New York, Plenum Press, p. 99–140.

Clayton, R.N., Friedman, I., Graf, D.L., Mayeda, T.K., Meents, W.F., and Shimp, N.F., 1966, The origin of saline formation waters, I. Isotopic composition: Journal of Geophysical Research, v. 71, p. 3869–3882.

Clifton, H.E., 1957, The carbonate concretions of the Ohio Shale: Ohio Journal of Science: v. 57, p. 114–124.

Coleman, M.L., 1993, Microbial processes: controls on the shape and composition of carbonate concretions: Marine Geology, v. 119, p. 127–140.

Coniglio, M., Myrow, P., and White, T., 2000, Stable carbon and oxygen isotope evidence of Cretaceous sea-level fluctuations recorded in septarian concretions from Pueblo, Colorado, USA: Journal of Sedimentary Research, v. 70, p. 700–714.

Cox, B.M., Gallois, R.W., and Sumbler, M.G., 1994, The stratigraphy of the BGS Hartwell Borehole, near Aylesbury, Buckinghamshire: Proceedings of the Geological Association, v. 105, p. 209–224.

Criss, R.E., Cooke, G.A., and Day, S.D., 1988, An organic origin for the carbonate concretions of the Ohio Shale: U.S. Geological Survey, Bulletin 1836, p. 1–21.

Dale, A., John, C.M., Mozley, P.S., Smalley, P.C., and Muggeridge, A.H., 2014, Time-capsule concretions: unlocking burial diagenetic processes in the Mancos Shale using carbonate clumped isotopes: Earth and Planetary Science Letters, v. 394, p. 30–37.

Dennis, K.J., and Schrag, D.P., 2010, Clumped isotope thermometry of carbonatites as an indicator of diagenetic alteration: Geochimica et Cosmochimica Acta, v. 74, p. 4110–4122.

Dennis, K.J., Affek, H.P., Passey, B.H., Schrag, D.P., and Eiler, J.M., 2011, Defining an absolute reference frame for "clumped" isotope studies of CO_2: Geochimica et Cosmochimica Acta, v. 75, p. 7117–7131.

Desrochers, A., and Al-Aasm, S., 1993, The formation of septarian concretions in Queen Charlotte Islands, B.C.: evidence for microbially and hydrothermally mediated reactions at shallow burial depth: Journal of Sedimentary Petrology, v. 63, p. 282–294.

Dix, G.R., and Mullins, H.T., 1987, Shallow, subsurface growth and burial alteration of Middle Devonian calcite concretions: Journal of Sedimentary Petrology, v. 57, p. 140–152.

Duck, R.W., 1995, Subaqueous shrinkage cracks and early sediment fabrics preserved in Pleistocene calcareous concretions: Geological Society of London, Journal, v. 152, p. 151–156.

Duff, K.L., 1975, Palaeoecology of a bituminous shale: the Lower Oxford Clay of Central England: Palaeontology, v. 18, p. 443–482.

Eagle, R.A., Schauble, E.A., Tripati, A., Tutken, T., Hulbert, C., and Eiler, J., 2010, Body temperatures of modern and extinct vertebrates from ^{13}C–^{18}O bonds abundances in bioapatite: National Academy of Sciences (U.S.A.), Proceedings, v. 107, p. 10,377–10,382.

Eagle, R.A., Tütken, T., Martin, T.S., Tripati, A.K., Fricke, H.C., Connely, M., Cifelli, R.L., and Eiler, J.M., 2011, Dinosaur body temperatures determined from isotopic (^{13}C–^{18}O) ordering in fossil biominerals: Science, v. 333, p. 443–445.

Eubukanson, E.J., and Kinghorn, R.R.F., 1985, Kerogen facies in the major Jurassic mudrock formations of southern England and their implication on the depositional environments of their precursors: Journal of Petroleum Geology, v. 8, p. 434–462.

Eubukanson, E.J., and Kinghorn, R.R.F., 1986, Maturity of organic matter in the Jurassic of southern England and its relation to the burial history of the sediments: Journal of Petroleum Geology, v. 9, p. 259–280.

Feistner, K.W.A., 1989, Petrographic examination and re-interpretation of concretionary carbonate horizons from the Kimmeridge Clay, Dorset: Geological Society of London, Journal, v. 146, p. 345–350.

Finnegan, S., Bergmann, K., Eiler, J.M., Jones, D.S., Fike, D.A., Eisenman, I., Hughes, N.C., Tripati, A.K., and Fischer, W.W., 2011, The magnitude and duration of Late Ordovician–Early Silurian glaciation: Science, v. 331, p. 903–906.

Gallois, R.W., and Cox, B.M., 1976, Stratigraphy of the Lower Kimmeridge Clay of Eastern England: Yorkshire Geological Society, Proceedings, v. 41, p. 13–26.

Gautier, D.L., 1982, Siderite concretions: indicators of early diagenesis in the Gammon Shale (Cretaceous): Journal of Sedimentary Petrology, v. 52, p. 859–871.

Gautier, D.L., and Claypool, G.E., 1984, Interpretation of methanic diagenesis in ancient sediments by analogy with process in modern diagenetic environments, *in* McDonald, D.A., and Surdam, R.C., eds., Clastic Diagenesis: American Association of Petro1eum Geologists, Memoirs, v. 37, p. 111–123.

Ghosh, P., Adkins, J., Affek, H., Balta, B., Guo, W., Schauble, E., Schrag, D., and Eiler, J., 2006a, ^{13}C–^{18}O bonds in carbonate minerals: a new kind of paleothermometer: Geochimica et Cosmochimica Acta, v. 70, p. 1439–1456.

Ghosh, P., Garzione, C.N., and Eiler, J.M., 2006b, Rapid uplift of the Altiplano revealed through ^{13}C–^{18}O bonds in paleosol carbonates: Science, v. 311, p. 511–515.

Green, P.F., 1989a, Thermal and tectonic history of the East Midlands shelf (onshore UK) and surrounding regions assessed by apatite fission track analysis: Geological Society of London, Journal, v. 146, p. 755–773.

Green, P.F., 1989b, Uplift and erosional history of Cleveland Basin and surrounding areas revealed by apatite fission track analysis [Abstract]: Washington D.C., 28th International Geological Congress, July 9–19, p. 585–586.

Gross, M.G., 1964, Variations in the ratios of diagenetically altered limestones in the Bermuda Islands: The Journal of Geology, v. 72, p. 170–194.

Haggart, J.W., Ward, P.D., Raub, T.D., Carter, E.S., and Kischvink, J.L., 2009, Molluscan biostratigraphy and paleomagnetism of Campanian strata, Queen Charlotte Islands, British Columbia: implications for Pacific coast North America biochronology: Cretaceous Research, v. 30, p. 939–951.

Hendry, J.P., Pearson, M.J., Trewin, N.H., and Fallick, A.E., 2006, Jurassic septarian concretions from NW Scotland record interdependent bacterial, physical and chemical processes of marine mudrock diagenesis: Sedimentology, v. 53, p. 537–565.

Hennessy, J., and Knauth, L.P., 1985, Isotopic variations in dolomite concretions of the Monterey Formation, California: Journal of Sedimentary Petrology, v. 55, p. 120–130.

Hounslow, M.W., 1997, Significance of localized pore pressures to the genesis of septarian concretions: Sedimentology, v. 44, p. 1133–1147.

Hudson, J.D., 1978, Concretions, isotopes and the diagenetic history of the Oxford Clay (Jurassic) of central England: Sedimentology, v. 25, p. 339–370.

Hudson, J.D., and Martill, D.M., 1994, The Peterborough Member (Callovian, Middle Jurassic) of the Oxford Clay Formation at Peterborough, UK: Geological Society of London, Journal, v. 151, p. 113–124.

Hudson, J.D., Coleman, M.L., Barreiro, B.A., and Hollingworth, N.T.J., 2001, Septarian concretions from the Oxford Clay (Jurassic, England, UK): involvement of original marine and multiple external pore fluids: Sedimentology, v. 48, p. 507–531.

Huntington, K.W., Wernicke, B.P., and Eiler, J.M., 2010, Influence of climate change and uplift on Colorado Plateau paleotemperatures from carbonate clumped isotope thermometry: Tectonics, v. 29, 19 p.

Huntington, K.W., Budd, D.A., Wernicke, B.P., and Eiler, J.M., 2011, Use of clumped-isotope thermometry to constrain the crystallization temperature of diagenetic calcite: Journal of Sedimentary Research, v. 81, p. 656–669.

Hyde, C., and Landy, R.A., 1966, Whewellite from septarian concretions near Milan, Ohio: American Mineralogist, v. 51, p. 228.

Irwin, H., Curtis, C., and Coleman, M., 1977, Isotopic evidence for source of diagenetic carbonates formed during burial of organic-rich sediments: Nature, v. 269, p. 209–213.

Irwin, H., 1979a, Chemical Diagenesis in an Organic Rich Sediment Sequence [PhD thesis]: University of Sheffield, 187 p.
Irwin, H., 1979b, On an environmental model for the type Kimmeridge Clay: a discussion: Nature, v. 279, p. 819.
Jorgensen, B.B., 1977, The sulfur cycle of a coastal marine sediment (Limfjorden, Denmark): Limnology and Oceanography, v. 22, p. 814–832.
Kim, S.-T., and O'Neil, J.R., 1997, Equilibrium and nonequilibrium oxygen isotope effects in synthetic carbonates: Geochimica et Cosmochimica Acta, v. 61, p. 3461–3475.
Lawrence, J.R., Drever, J.I., Anderson, T.F., and Brueckner, H.K., 1979, Importance of alteration of volcanic material in the sediments of Deep Sea Drilling site 323: chemistry, $^{18}O/^{16}O$ and $^{87}Sr/^{86}Sr$: Geochimica et Cosmochimica Acta, v. 43, p. 573–588.
Lawrence, J.R., and Gieskes, J.M., 1981, Constraints on water transport and alteration in the oceanic crust from isotopic composition of pore water: Journal of Geophysical Research, v. 86, p. 7924–7934.
Lohmann, K.C, 1988, Geochemical patterns of meteoric diagenetic systems and their application to studies of paleokarst, *in* James, N.P., and Choquette, P.W., eds., Paleokarst: New York, Springer-Verlag, p. 58–80.
Loyd, S.J., Corsetti, F.A., Eiler, J.M., and Tripati, A.K., 2012a, Determining the diagenetic conditions of concretion formation: assessing temperatures and pore waters using clumped isotopes: Journal of Sedimentary Research, v. 82, p. 1006–1016.
Loyd, S.J., Berelson, W.M., Lyons, T.W., Hammond, D.E., and Corsetti, F.A., 2012b, Constraining pathways of microbial mediation for carbonate concretions of the Miocene Monterey Formation using carbonate-associated sulfate: Geochimica et Cosmochimica Acta, v. 78, p. 77–98.
Loyd, S.J., Dickson, J.A.D., Scholle, P.A., and Tripati, A.K., 2013, Extensive, uplift-related and non-fault-controlled spar precipitation in the Permian Capitan Formation: Sedimentary Geology, v. 298, p. 17–27.
Marshall, J.D., 1982, Isotopic composition of displacive fibrous calcite veins: reversals in pore-water composition trends during burial diagenesis: Journal of Sedimentary Petrology, v. 52, p. 615–630.
Marshall, J.D., and Ashton, M.A., 1980, Isotopic and trace element evidence for submarine lithification of hardgrounds in the Jurassic of eastern England: Sedimentology, v. 27, p. 271–290.
Martill, D.M., and Hudson, J.D., 1989, Injection clastic dykes in the Lower Oxford Clay (Jurassic) of central England: relationship to compaction and concretion formation: Sedimentology, v. 36, p. 1127–1133.
McLimans, R.K., and Videtich, P.E., 1989, Diagenesis and burial history of Great Oolite Limestone, Southern England: American Association of Petro1eum Geologists, Bulletin, v. 73, p. 1195–1205.
Morris, K.A., 1980, Comparison of major sequences of organic-rich mud deposition in the British Jurassic: Geological Society of London, Journal, v. 137, p. 157–170.
Morton, R.A., and Land, L.S., 1987, Regional variations in formation water chemistry, Frio Formation (Oligocene), Texas Gulf Coast: American Association of Petro1eum Geologists, Bulletin, v. 71, p. 191–206.
Mozley, P.S., 1989, Complex compositional zonation in concretionary siderite: implications for geochemical studies: Journal of Sedimentary Petrology, v. 59, 815–818.
Mozley, P.S., 1996, The internal structure of carbonate concretions in mudrocks: a critical evaluation of the conventional concentric model of concretion growth: Sedimentary Geology, v. 103, p. 85–91.
Mozley, P.S., and Burns, S.J., 1993, Oxygen and carbon isotopic composition of marine carbonate concretions: an overview: Journal of Sedimentary Petrology, v. 63, p. 73–83.
Newberry, J.S., 1873, Geological structure of Ohio-Devonian system: Ohio Geological Survey, Reports, v. 1, p. 140–167.
Palmer, M.R., and Elderfield, H., 1985, Sr isotope composition of seawater over the past 75 Myr: Nature, v. 314, p. 526–528.
Passey, B.H., and Henkes, G.A., 2012, Carbonate clumped isotope bond reordering and geospeedometry. Earth and Planetary Science Letters, v. 351–352, p. 223–236.
Passey, B.H., Levin, N.E., Cerling, T.E., Brown, F.H., and Eiler, J.M., 2010, High-temperature environments of human evolution in East Africa based on bond ordering in paleosol carbonates: National Academy of Sciences (U.S.A.), Proceedings, v. 107, p. 11245–11249.
Penn, I.E., Cox, B.M., and Gallois, R.W., 1986, Towards precision in stratigraphy: geophysical log correlation of Upper Jurassic (including Callovian) strata of the Eastern England shelf: Geological Society of London, Journal, v. 143, p. 381–410.
Perry, E.A., Gieskes, J.M., and Lawrence, J.R., 1976, Mg, Ca and $^{18}O/^{16}O$ exchange in the sediment–pore water system Hole 149, DSDP: Geochimica et Cosmochimica Acta, v. 40, p. 413–423.
Pratt, B.R., 2001, Septarian concretions: internal cracking caused by synsedimentary earthquakes: Sedimentology, v. 48, p. 189–213.
Raiswell, R., 1971, The growth of Cambrian and Liassic concretions: Sedimentology, v. 17, p. 147–171.
Raiswell, R., and Fisher, Q.J., 2000, Mudrock-hosted carbonate concretions: a review of growth mechanisms and their influence on chemical and isotopic composition: Geological Society of London, Journal, v. 157, p. 239–251.
Sass, E., Bein, A., and Almogi-Labin, A., 1991, Oxygen-isotope composition of diagenetic calcite in organic-rich rocks: evidence for ^{18}O depletion in marine anaerobic porewater: Geology, v. 19, p. 839–842.
Scotchman, I.C., 1984, Diagenesis of the Kimmeridge Clay Formation [PhD thesis]: University of Sheffield, 531 p.
Scotchman, I.C., 1989, Diagenesis of the Kimmeridge Clay Formation, onshore UK: Geological Society of London, Journal, v. 146, p. 285–303.
Scotchman, I.C., 1991, The geochemistry of concretions from the Kimmeridge Clay Formation of southern and eastern England: Sedimentology, v. 38, p. 79–106.
Selles-Martínez, J., 1996, Concretion morphology, classification and genesis: Earth-Science Reviews, v. 41, p. 177–210.
Sellwood, B.W., Shepherd, T.J., Evans, M.R., and James, B., 1989, Origin of late cements in oolitic reservoir facies: a fluid inclusion and isotopic study (Mid-Jurassic, Southern England): Sedimentary Geology, v. 61, p. 223–237.
Siegel, D.I., Chamberlain, S.C., and Dossert, W.P., 1987, The isotopic and chemical evolution of mineralization in septarian concretions: evidence for episodic paleohydrologic methanogenesis: Geological Society of America, Bulletin, v. 99, p. 385–394.
Swart, P.K., Burns, S.J., and Leder, J.J., 1991, Fractionation of the stable isotopes of oxygen and carbon in carbon dioxide during the reaction of calcite with phosphoric acid as a function of temperature and technique: Chemical Geology, Isotope Geoscience Section, v. 86, p. 89–96.
Thyne, G.D., and Boles, J.R., 1989, Isotopic evidence for origin of the Moeraki septarian concretions, New Zealand: Journal of Sedimentary Petrology, v. 59, p. 272–279.
Tomkeieff, S.I., 1927, On the mode and origin of certain kaolinite-bearing nodules in the Coal Measures: Proceedings of the Geological Association, v. 38, p. 518–547.
Tripati, A.K., Eagle, R.A., Thiagarajan, N., Gagnon, A.C., Bauch, H., Halloran, P.R., and Eiler, J.M., 2010, ^{13}C–^{18}O isotope signatures and "clumped isotope" thermometry in foraminifera and coccoliths: Geochimica et Cosmochimica Acta, v. 74, p. 5697–5717.
Tyson, R.V., Wilson, R.C.L., and Downie, C., 1979, A stratified water column environment model for the type Kimmeridge Clay: Nature, v. 277, p. 377–380.
Urey, H.C., 1947, The thermodynamic properties of isotopic substances: Chemical Society of London, Journal, v. 1, p. 562–581.
Veizer, J., Ala, D., Azmy, K., Bruckschen, P., Buhl, D., Bruhn, F., Carden, G.A.F., Diener, A., Ebneth, S., Godderis, Y., Jasper, T., Korte, C., Pawellek, F., Podlaha, O.G., and Strauss, H., 1999, $^{87}Sr/^{86}Sr$, $\delta^{13}C$ and $\delta^{18}O$ evolution of Phanerozoic seawater: Chemical Geology, v. 161, p. 59–88.
Wynne, P.J., Irving, E., Maxson, J.A., and Kleinspehn, K.L., 1995, Paleomagnetism of the Upper Cretaceous strata of Mount Tatlow: evidence for 3000 km of northward displacement of the eastern Coast Belt, British Columbia: Journal of Geophysical Research, v. 100, p. 6073–6091.
Wignall, P.B., 1989, Sedimentary dynamics of the Kimmeridge Clay: tempests and earthquakes: Geological Society of London, Journal, v. 146, p. 273–284.
Wignall, P.B., and Myers, K.J., 1988, Interpreting benthic oxygen levels in mudrocks: a new approach: Geology, v. 16, p. 452–455.
Zachos, J., Pagani, M., Sloan, L., Thomas, E., and Billups, K., 2001, Trends, rhythms, and aberrations in global climate 65 Ma to present: Science, v. 292, p. 686–693.

Received 18 November 2013; accepted 2 September 2014.